Journal of Hydrology 585 (2020) 124780

Contents lists available at ScienceDirect

Journal of Hydrology

journal homepage: www.elsevier.com/locate/jhydrol

Research papers

Large-scale baseflow index prediction using hydrological modelling, linear and multilevel regression approaches

Junlong Zhang[a], Yongqiang Zhang[b,*], Jinxi Song[c,d,*], Lei Cheng[e], Pranesh Kumar Paul[b], Rong Gan[f], Xiaogang Shi[g], Zhongkui Luo[h], Panpan Zhao[i]

[a] College of Geography and Environment, Shandong Normal University, Jinan 250358, China
[b] Key Laboratory of Water Cycle and Related Land Surface Processes, Institute of Geographic Sciences and Natural Resources Research, Chinese Academy of Sciences, Beijing 100101, China
[c] Shaanxi Key Laboratory of Earth Surface System and Environmental Carrying Capacity, College of Urban and Environmental Sciences, Northwest University, Xi'an 710127 China
[d] State Key Laboratory of Soil Erosion and Dryland Farming on the Loess Plateau, Institute of Soil and Water Conservation, Chinese Academy of Sciences, Yangling 712100, China
[e] State Key Laboratory of Water Resources and Hydropower Engineering Science, Wuhan University, Wuhan 430072, China
[f] School of Life Sciences, University of Technology Sydney, NSW 2007, Australia
[g] School of Interdisciplinary Studies, University of Glasgow, Dumfries DG1 4ZL, UK
[h] College of Environmental and Resource Sciences, Zhejiang University, Hangzhou 310058, China
[i] Institute of Water Conservancy, North China University of Water Resource and Electric Power, Zhengzhou 450045, China

ARTICLE INFO

This manuscript was handled by Marco Borga, Editor-in-Chief, with the assistance of Eylon Shamir, Associate Editor

Keywords:
Baseflow separation
BFI
Multilevel regression
Hydrological models
Linear regression

ABSTRACT

Baseflow is critical for water balance budget, water resources management, and environmental evaluation. Prediction of baseflow index (BFI), the ratio of baseflow to total streamflow, has a great significance in unravelling the baseflow characteristics for large scale trajectory. Therefore, this study compares BFI predictive performance derived from a new multilevel regression approach along with two other commonly used approaches: hydrological modelling (SIMHYD, a simplified version of the HYDROLOG model, and Xinanjiang model), and linear regression (traditional linear regression, and alternative traditional regression considers the second-order interaction). The multilevel regression approach does not only group the catchments into the four climate zones (arid, tropics, equiseasonal and winter rainfall), but also considers inter-catchment and inter-climate zone variances. Likewise, calibration and two regionalisation techniques namely spatial proximity and integrated similarity are used to obtain the BFI from hydrological modelling approach. Correspondingly, the traditional linear regression technique estimates BFI establishing linear regressions between catchment attributes and four climate zones. Then, all the three approaches are evaluated against combined average estimation from four well-parameterised baseflow separation methods (Lyne-Hollick (LH), United Kingdom Institute of Hydrology (UKIH), Chapman-Maxwell (CM) and Eckhardt (ECK)) at 596 catchments across Australia for 1980–2012. The findings show that the multilevel regression has greatly improved the performance of BFI prediction in comparison to other methods. In particular, the two calibrated and regionalised hydrological models perform worst in predicting BFI with a Nash-Sutcliffe Efficiency (NSE) of −8.44 and −2.58 along with an absolute percent bias (PBIAS) of 81% and 146% (overestimation of baseflow), respectively. However, the traditional linear regression remains in intermediate position with the NSE of 0.57 and bias of 25. In addition, alternative traditional regression also shows very close proximity. In contrast, the multilevel regression approach shows the best performance with the NSE of 0.75 and bias of 19%. The study also demonstrates that the multilevel regression approach can improve BFI prediction, and shows potential for being used in the prediction of other hydrological signatures in large-scale.

* Corresponding authors. Key Laboratory of Water Cycle and Related Land Surface Processes, Institute of Geographic Sciences and Natural Resources Research, Chinese Academy of Sciences, Beijing 100101, China.
E-mail addresses: zhangyq@igsnrr.ac.cn (Y. Zhang), jinxisong@nwu.edu.cn (J. Song).

https://doi.org/10.1016/j.jhydrol.2020.124780
Received 12 August 2019; Received in revised form 16 February 2020; Accepted 27 February 2020
Available online 29 February 2020

1. Introduction

Baseflow is the water flow from upstream aquifers/groundwater, when the recharge (e.g., precipitation or other artificial water supplies) is ceased (Brutsaert and Lopez, 1998; Brutsaert, 2005). Therefore, it is considered as an important hydrogeological characteristic for a catchment (Knisel, 1963). Correspondingly, baseflow index (BFI) is the average rate of baseflow to streamflow over a long period of time (Piggott et al., 2005; Partington et al., 2012). As a result, accurate estimation of baseflow and BFI has a profound influence on assessing catchment water scarcity, during drought periods (Brutsaert, 2005; Zhang et al., 2014; Miller et al., 2016). To be precise, it is critical for water budgets (Abdulla et al., 1999), water management strategies (Lacey and Grayson, 1998), engineering design (Meynink, 2011), and other related environmental issues (Spongberg, 2000; Miller et al., 2014).

As a consequence, various methods have been developed to separate baseflow from gauged streamflow (Lyne and Hollick, 1979; Rice and Hornberger, 1998; Spongberg, 2000; Furey and Gupta, 2001; Eckhardt, 2005; Tularam and Ilahee, 2008; Lott and Stewart, 2016). They are mainly categorized into tracer-based and non-tracer methods (Gonzales et al., 2009). The tracer-based method is applied to experimental catchments due to the high consumption of both experimental time and materials (Koskelo et al., 2012). To overcome the issue, several non-tracer methods have been developed over the years. Digital filtering technique is the major non-tracer based method which is widely used owing to high efficiency and repeatability (Arnold et al., 1995; Zhang et al., 2017). More importantly, they perform well when the digital filtering parameters (i.e., recession constant and maximum baseflow index) are appropriately estimated (Zhang et al., 2017). Besides, they are only applicable for catchments with streamflow observations. Therefore, for ungauged catchments, hydrological models and regression approaches can be used to separate baseflow from total streamflow. Since, their accuracy is largely unknown, they can be evaluated against combined estimates from the non-tracer based methods at gauged catchments. For reducing uncertainty of baseflow estimates, four non-tracer based methods namely Lyne-Hollick (LH) (Lyne and Hollick, 1979), United Kingdom Institute of Hydrology (UKIH) (Gustard et al., 1992), Chapman-Maxwell (CM) (Chapman and Maxwell, 1996) and Eckhardt (ECK) (Eckhardt, 2005) are selected.

However, most hydrological models include a baseflow generation component (Luo et al., 2012; Stoelzle et al., 2015; Gusyev et al., 2016). These models can be divided into two groups. One group considers baseflow as a linear recession process for groundwater reservoir, including SIMHYD (simplified version of the HYDROLOG model) (Chiew and McMahon, 1994; Zhang et al., 2016), 1LBY (Abdulla et al., 1999; Stoelzle et al., 2015), and HBV (Ferket et al., 2010) models. The other group takes baseflow into account as a non-linear recession process including Xinanajing (Zhang and Chiew, 2009), PDM (Ferket et al., 2010) and ARNO (Abdulla et al., 1999) models. It is clear that the BFI derived from those hydrological models have large uncertainties, since the baseflow and total flow are greatly varied with the model structures, model calibration and parameterisation schemes (Beven and Freer, 2001). Therefore, for ungauged catchments, their reliability always remains a question. However, Zhang et al. (2013) conclude, based on review, that regression models are easy to implement and capable of estimating baseflow with reasonable accuracy at ungauged catchments.

This method first establishes linear regressions between physical characteristics of catchment (i.e., descriptors) and BFI is obtained from the gauged catchments and then conduct the prediction for ungauged catchments (Bloomfield et al., 2009; Beck et al., 2013). For the selection of predictors, several studies have considered geological characteristics, such as soil properties, to have important control over catchment BFI (Brandes et al., 2005; van Dijk, 2010). A few studies have used meteorological indices, such as mean annual precipitation and mean annual potential evaporation as variables to predict BFI (van Dijk, 2010; Beck et al., 2013). Other similar studies have used mean annual precipitation, slope and proportion of grassland as predictors of BFI (Haberlandt et al., 2001; Brandes et al., 2005; Mazvimavi et al., 2005; Gebert et al., 2007; Bloomfield et al., 2009; van Dijk, 2010). However, one major limitation of the linear regression approach is that it uses constant value of parameters to predict BFI, and cannot handle issues at different spatial scales (Qian et al., 2010), thus high uncertainties may arise in BFI prediction for catchments located in a wide range of climate and geological regimes.

This limitation can be overcome by using multilevel regression approach (Qian et al., 2010; Luo et al., 2015). It provides a robust tool to establish the relationships between BFI and catchment attributes. The basic idea of this approach is that higher-level variables vary within lower-level variables (Berk and De Leeuw, 2006). This approach can also handle the variables with various solutions using hierarchical structure (Dudaniec et al., 2013). It has been extensively used to understand the interplay of ecosystem dynamics (i.e., carbon cycle across different ecosystems and N_2O emissions from farmlands) (Carey, 2007; McMahon and Diez, 2007; Luo et al., 2015). In addition, some studies are used multilevel model to address the hydrological related issues (i.e., to predict the flow duration curve (Booker and Snelder, 2012), to estimate the impacts of climate change to flow intermittency (Reynolds et al., 2015) and effects of flow connectivity to dissolved organic matter (Granados et al., 2020)). However, no study has been reported to use this approach for predictions of BFI. This study, for the first time, explores the possibility of using multilevel regression to predict BFI across widely distributed Australian catchments that cover various climate and geological regions.

At this juncture, the main aim of this study is to evaluate various methods in predicting BFI. To achieve this goal, we compare the three BFI prediction methods (hydrological modelling, linear regression and multilevel regression approaches) against combined average estimates from four non-tracer baseflow separation methods. The specific objectives of this study are:

i. To obtain “benchmark” BFI using the four non-tracer baseflow methods LH, UKIH, CM and ECK) for 596 Australian catchments (Fig. 1);
ii. To introduce the multilevel regression approach for BFI predictions across large regions; and
iii. To assess relative merits of the three approaches for BFI predictions;

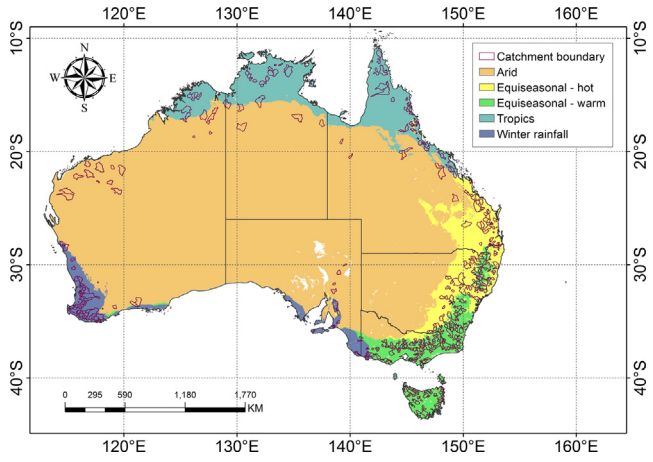

Fig. 1. The location of 596 selected unregulated small catchments in this study and climate classification based on Köppen-Geiger (2006) classification schemes in Australia.

2. Data sources

2.1. Streamflow

Daily observed data (Q) (1975–2012) for 596 catchments across Australia (Fig. 1) have been collated by Zhang et al. (2013) to assess the three methods (hydrological modelling, linear regression, and multilevel regression) for predicting BFI. Following criteria are used to select the catchment streamflow data:

i. The catchment area is small enough to minimize routing process influence (varying between 50 and 5000 km^2);
ii. Streamflow is not subject to dam or reservoir regulations;
iii. The catchment is non-nested;
iv. The catchment is not subject to major impacts of irrigation and intensive land use; and
v. The observed streamflow, containing at least ten-year (> 3652 days) daily observations, with acceptable data quality according to a consistent Australian standard (Viney et al., 2011).

2.2. Climate zones and catchment attributes

The climate zones are regarded as higher-level predictors due to the influence on the predictors' effect size and direction (Gelman and Hill, 2006). To be specific, the Australian continent is classified into five climate zones (arid, equiseasonal-hot, equiseasonal-warm, tropics and winter rainfall) based on Köppen-Geiger classification schemes (Kottek et al., 2006). Herein equiseasonal-hot and equiseasonal-warm are combined as one climate zone. The numbers of selected catchments within arid, equiseasonal, tropics, and winter rainfall climate zones are 38, 385, 83, and 90, respectively.

On the other hand, the catchment attributes, regarded as lower-level predictors, including climate (Mean annual precipitation, P, mean annual potential evaporation, Etp), topographical (Mean elevation and Mean slope), soil (Available soil water holding capacity) and land cover (Forest cover ratio) characteristics are implemented in the linear regression and multilevel regression approaches to estimate BFI. The catchment attributes are collected from the dataset collated by Zhang et al. (2013). The abbreviation for each catchment attribute and summary is shown in Tables 1 and 2 respectively.

2.3. Forcing data for hydrological modelling

The Xinanjiang and SIMHYD models are driven by 0.05° resolution (~5 km) daily meteorological data (precipitation, maximum temperature, minimum temperature, incoming solar radiation, and actual vapour pressure) from 1975 to 2012, obtained from the Scientific Information for Land Owners (SILO) Data Drill of the Queensland Department of Natural Resources and Water (www.nrw.gov.au/silo). There are about 4600-point observations across Australia used for interpolation to obtain the SILO data. To have more details, please consult Jeffrey et al. (2001). The daily and monthly gridded precipitation data are obtained from the ordinary kriging method, whereas other gridded climate variables are obtained using the thin plate smoothing spline technique. Cross-validation results indicate good data quality with the mean absolute error of the Jeffrey interpolation (Jeffrey et al., 2001) for maximum daily air temperature, minimum daily air temperature, vapour pressure, and precipitation being 1.0 °C, 1.4 °C, 0.15 kPa and 12.2 mm/month, respectively.

Along with the climate forcing data, the two models also require remotely sensed leaf area index (LAI), land cover and albedo data as inputs in the Penman–Monteith–Leuning model to calculate actual evapotranspiration (ET_a) (Leuning et al., 2009; Zhang et al., 2010). LAI data from 1981 to 2011 are obtained from Advanced Very High Resolution Radiometer (AVHRR) in Boston University (Zhu et al., 2013). The temporal resolution and spatial resolution are of six months and ~8 km, respectively. The Moderate Resolution Imaging Spectroradiometer (MODIS) land cover product (2000–2001) is used to estimate aerodynamic conductance, obtained from the Oak Ridge National Laboratory Distributed Active Archive Center (Friedl et al., 2010). The dataset has 17 vegetation classes, which are defined according to the International Geosphere-Biosphere Programme (IGBP). The albedo data, obtained from the 8-day MODIS MCD43B bidirectional reflectance distribution function product at 1 km resolution, are used to calculate net radiation. All the forcing data are re-projected and resampled using nearest neighbour approach to obtain 0.05° gridded data.

Table 1
Catchment attributes and indicators used in present study.

Catchment attributes	Notation	Unit
Area	A	km^2
Mean elevation	H	m
Mean slope	S	%
Mean annual precipitation	P	mm y^{-1}
Mean annual potential evaporation	E_{tp}	mm y^{-1}
Forest cover ratio	F	%
Available soil water holding capacity in top soil	K_{st}	mm/hr

Table 2
Summary statistics of the catchment information including topographic, climate, geological elements and forest cover ratio in 596 catchments across Australia. The abbreviations of catchment attributes are introduced in Table 1.

	A	H	S	P	E_{tp}	F	K_{st}
Max	4805.93	1350.97	16.02	3683.76	2237.88	0.91	507.28
Min	50.34	37.61	0.15	241.77	905.88	0.01	5.54
Mean	646.06	433.21	4.48	981.12	1384.12	0.49	158.83
25th	153.31	223.18	1.90	727.42	1155.48	0.34	105.42
50th	346.15	347.00	3.60	885.32	1294.93	0.52	161.17
75th	710.13	604.29	6.71	1162.30	1536.10	0.67	201.90

3. Models and algorithms

3.1. Hydrological models

We have selected two hydrological models (i.e., more process-based) SIMHYD and Xinanjiang because: (1) they are widely used in various climate regimes, and (2) they have different baseflow generation mechanisms which consider linear and non-linear recession for groundwater reservoir processes, respectively. Between them, SIMHYD has been widely applied in runoff simulations and regionalization studies (Chiew et al., 2009; Vaze and Teng, 2011; Li and Zhang, 2016; Zhang et al., 2016). Four water stores are used in this model to describe hydrological processes, namely the interception store, soil moisture store, groundwater store and channel store (Chiew and McMahon, 2002). Detailed model structure is available in Chiew and McMahon (1994). However, the modified SIMHYD model by Zhang and Chiew (2009), which uses remote sensing data and contains nine model parameters, is used in this study.

On the other hand, the Xinanjiang model (Zhao, 1992) has been widely used for humid and semi-arid regions including Australian catchments (Li et al., 2009; Lü et al., 2013; Yao et al., 2014). This model reproduces runoff by describing three hydrological processes including ET_a, runoff generation, and runoff routing. Details of the Xinanjiang model are available in Zhao (1992) as well as in Zhang and Chiew (2009). Here we use the modified Xinanjiang model proposed by Zhang and Chiew (2009), in which ET_a is estimated using remotely sensed LAI data and the number of model parameters has been reduced from 14 to 12. These two hydrological models first simulate daily baseflow and daily total streamflow time series, which are then aggregated as mean annual baseflow and mean annual total streamflow, respectively.

Finally, the BFI is estimated using the mean annual baseflow divided by the mean annual total streamflow.

Based on the BFI defined in the previous paragraph, we estimate baseflow, total streamflow and BFI in three ways: calibration, regionalisation from spatial proximity, and regionalisation from integrated similarity. The daily observed streamflow data from 1975 to 2012 (1975–1979 as warm up period) are used in calibration (1980–2012). Herein, a short description of these three kinds of estimates is given below.

A global optimisation method (a genetic algorithm) from the global optimisation toolbox in MATLAB (MathWorks, 2006) is used to calibrate the model parameters for each catchment (Zhang and Chiew, 2009). This optimiser uses 400 populations and the maximum generation of 100, for searching the optimum point, which converges at approximately 50 generations of searching. More information is found in Zhang et al. (2018). The model calibration is conducted by maximising the Nash-Sutcliffe Efficiency of the daily square-root-transformed runoff data (NSEsqrt) and minimising model bias (Li and Zhang, 2017).

Then, for spatial cross-validations, two regionalisation approaches, spatial proximity and integrated similarity approaches are used (Zhang and Chiew, 2009). The spatial proximity approach uses the parameter set from geographically closest catchment considering as the donor catchment to predict runoff at the target catchments. The integrated similarity approach derives parameter set for the objective catchment by combing the spatial proximity and physical similarity approaches, where the physical similarity approach adopts parameter set from the donor catchment. The two regionalisation approaches take five-donor combined mean for prediction, as recommended by Zhang and Chiew (2009) and Li and Zhang (2017).

3.2. Linear regression and multilevel regression approaches

In linear regression (1980–2012), BFI is predicted using one set of parameters for all catchments. The details are:

$$BFI = N(\alpha + \beta \cdot X, \varepsilon) \tag{1}$$

where, BFI is the baseflow index for each catchment, N denotes the normal distribution function, α is the intercept, β is the slope, X represents the variables (i.e., catchment attributes), and ε is the variance. However, this model ignores the potentially different effects of the same variable on BFI across different climatic zones. Therefore, the α and β are constant irrespective of the climatic zone (Abebe and Foerch, 2006; Longobardi and Villani, 2008; Bloomfield et al., 2009). But, baseflow processes are not only influenced by local catchment attributes, but also by geographical backgrounds (i.e., climate zones). However, the constant parameters (Eq. (1)) are not adequate to reflect the catchment characteristics. Therefore, BFI prediction may be improved by taking the influences derived from various catchment attributes and connection between different climate zones into account i.e. their cross-level interactions at different spatiotemporal scales (Qian et al., 2010).

At this juncture, we introduce multilevel regression (1980–2012) to overcome the limitation, due to its capability of capturing the cross-level interactions (Gelman and Hill, 2006; Qian et al., 2010; Luo et al., 2015). BFI in general associates with the climate variables (mean annual precipitation and mean annual potential evapotranspiration) and terrain attributes (area, elevation, slope, land cover and available soil water holding capacity of top soil) in each catchment (i.e., $i = 1, 2, 3, \ldots, 596$). Furthermore, the effects of these predictors on BFI are assumed varying with climate zones: arid, tropics, equiseasonal and winter rainfall (i.e., $j = 1, 2, 3, 4$). The BFI for catchment in each climatic class can be expressed as:

$$BFI_{ji} = N(\alpha + \beta \cdot X_{ji}, \varepsilon_j), \quad i \in (1, 2, 3, \ldots, 596) \tag{2}$$

where, BFI_{ji} is the baseflow index for the i^{th} catchment in the j^{th} climate zone. N is the normal distribution function, α is the intercept, β is slope, X is the variables (i.e., catchment attributes), and ε is the variance in each subset. For the linear regression approach, we firstly build the linear regression model for total data and sub-data for each climate class. Secondly, we consider second-order interactions through alternative traditional regression. In this study, the all subsets procedure (Wasserman and Sudjianto, 1994) in R package of "leaps" (https://cran.r-project.org/web/packages/leaps/index.html) is used as the platform to determine the parameters and then the R basic function lm () is used to build the linear regression model to predict BFI for total data and subset data (each climate zone) separately (denotes the traditional linear regression). To compare the model performance fairly, the alternative "traditional regression" (denotes alternative traditional regression) considers the second-order interaction also is used to build the model using rFSA package in R (https://cran.r-project.org/web/packages/rFSA/index.html) for total data. This tool provides a Feasible Solution Algorithm to find a set of feasible solutions for a statistical model of a specific form that includes second-order interactions between climate class and some catchment attributes (Lambert et al., 2018).

In comparison to the traditional linear regression approach, the multilevel regression approach has the hierarchical structure, and allows the assessment of the variation in model coefficients across groups (e.g., climatic zones) and accounts for group-level variation when estimates individual-level coefficients. This model is a two-stage regression, estimating the effects for each individual group in stage one (within-group), and then fitting interactive group effects on group-level predictors in stage two (between-group). The final regression coefficients link parameters from both levels which contain catchment attributes (lower-level) and climate zones (higher-level), including varying coefficients (both the intercept and slope vary by the group) (Gelman and Hill, 2006). For the application, there are two data matrices are used to conduct the multilevel regression, one data matrix is an individual catchment data matrix, and another is the classification of climate zones as the group index variable. The details of the approach are elaborated as follows:

$$BFI_i \tilde{N}(\alpha_{j[i]} + \beta_{j[i]} \cdot X_i, \sigma^2_{BFI}), \quad i = 1, 2, 3, \ldots, 596, \tag{3}$$

where, X_i is the catchment attributes for each basin, and its intercepts and slopes are decomposed into α and β terms for different climate zones,

$$\begin{pmatrix} \alpha_j \\ \beta_j \end{pmatrix} \sim N\left(\begin{pmatrix} \mu_\alpha \\ \mu_\beta \end{pmatrix}, \begin{pmatrix} \sigma_\alpha^2 & \rho\sigma_\alpha\sigma_\beta \\ \rho\sigma_\alpha\sigma_\beta & \sigma_\beta^2 \end{pmatrix} \right), \quad j = 1, 2, 3, 4, \tag{4}$$

where, μ_α and σ_α are the mean and standard deviation of variable intercept α; μ_β and σ_β are the mean and standard deviation of variable slope β; ρ is the correlation coefficients between the two variables α_j and β_j. The Eq. (3) is rearranged as a block matrix of

$$A \sim N(\mu, \sigma) \tag{5}$$

The details of Eq. (5) are described as:

$$A = \begin{pmatrix} \alpha_j \\ \beta_j \end{pmatrix}, \quad \mu = \begin{pmatrix} \mu_\alpha \\ \mu_\beta \end{pmatrix}, \quad \sigma = \begin{pmatrix} {\sigma_\alpha}^2 & \rho\sigma_\alpha\sigma_\beta \\ \rho\sigma_\alpha\sigma_\beta & {\sigma_\beta}^2 \end{pmatrix} \tag{6}$$

Then, the Eq. (4) is calculated individually by:

$$\alpha_j \sim N(\mu_\alpha, {\sigma_\alpha}^2) \tag{7}$$

$$\beta_j \sim N(\mu_\beta, {\sigma_\beta}^2) \tag{8}$$

However, the density function of the normal distribution N is (for example, α variable):

$$f(\alpha_j) = \frac{1}{\sqrt{2\pi}\sigma_\alpha} e^{-\frac{(\alpha_j - \mu_\alpha)^2}{2{\sigma_\alpha}^2}} \tag{9}$$

This model considers variation in the values of α_j and β_j along with a between-group correlation parameter ρ (Gelman and Hill, 2006; Qian

et al., 2010). In essence, there is a separate regression model for each climate zone with the coefficients estimated by the weighted average of pooled (which do not consider groups) and unpooled (which consider each group separately) estimates, i.e. partial pooling. When fitting the model, each predictor X is standardized using *z-scores*:

$$z - scores = \frac{X - mean(X)}{2SD(X)} \tag{10}$$

where *SD* is the standard deviation. Herein, the "lmer" function in R package of "lme4" (https://cran.r-project.org/web/packages/ lme4/index.html) is used to perform the multilevel regression analysis. To have a fair comparison, the multilevel regression and the linear regression with climate units are compared. This can evaluate the relative merits of the multilevel regression considering the interactive group effects.

3.3. Baseflow separation algorithm for preparation of benchmark BFI

The benchmark BFI data are estimated using four widely used baseflow separation methods namely LH (Lyne and Hollick, 1979), UKIH (Gustard et al., 1992), CM (Chapman and Maxwell, 1996) and ECK (Eckhardt, 2005). The successful use of the digital filter methods mainly depends on estimation of the recession constant and maximum baseflow index (Zhang et al., 2017). This study has used the Automatic Baseflow Identification Technique (ABIT) for the recession analysis, developed by Cheng et al. (2016) based on the recession theory proposed by Brutsaert and Nieber (1977). The recession points selected, in this method, dominantly consist of baseflows (Cheng et al., 2016). The method plots dQ/dt against Q with the 5% lower envelope, which represents the slowest recession rate (Fig. 2). Therefore, BFI estimated from the digital filter methods is physically meaningful and can reflect cumulative baseflow processes.

Besides, Fig. 3 shows that the four baseflow separation methods are well correlated (with R^2 ranging from 0.76 to 0.97). However, the BFI estimated from LH and CM is noticeably higher than that estimated from ECK and UKIH. In order to minimize uncertainties raised from the four methods, we use their output average as a benchmark (denoted as 'the benchmark BFI') to evaluate the performance of hydrological modelling and regression approaches (Jung et al., 2010; Cheng et al., 2017).

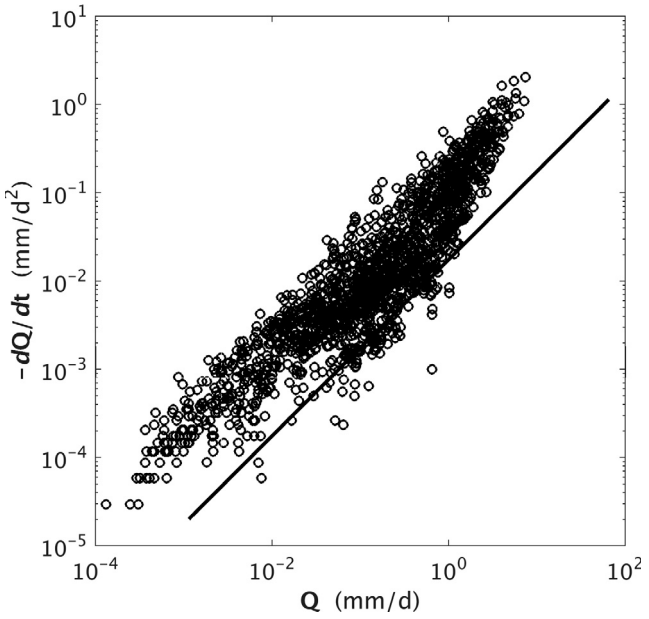

Fig. 2. Estimation of the recession constant (Log ($-dQ/dt$) versus log (Q)) using automated baseflow identification technique (ABIT) for Endeavour catchment (station ID 107001). The black line is 5% lower envelope line has a slope 0.983 and the estimate of the characteristic drainage time scale K = 57.1 days.

3.4. Leave-one-out cross-validations

We apply leave-one-out cross-validation to assess the ability of the two regression approaches to predict BFI in 'ungauged' catchments where the streamflow data are unavailable. This cross-validation is widely used since it can provide an almost unbiased estimate of the probability of test error in model selection (Cawley and Talbot, 2003), and would be more stable and more resilient to irreducible errors in each validation (Zhang et al., 2018). In the leave-one-out cross-validation, (1) each catchment is left out in turn, and is purposefully treated as "ungauged"; (2) a predictive relationship is then developed using data from the remaining catchments; and (3) finally, the relationship is used to predict the baseflow index for the catchment not used in developing the relationship. For each of the 596 catchments, the data from other 595 catchments are used to predict its BFI. This procedure is repeated over all 596 catchments. This cross-validation procedure explores the transferability of the two regression approaches from known catchments to the ungauged and particularly evaluates the information of the between-catchments.

4. Model evaluation

4.1. Bias

The absolute percentage bias was used to evaluate model performance, which is calculated as:

$$Bias = \left| \frac{\sum_{i=1}^{n} (BFI_s - BFI_o)}{\sum_{i=1}^{n} BFI_o} \times 100 \right| \tag{11}$$

where BFI_o is the benchmark BFI derived using the combined average from the four non-tracer baseflow separation approaches (i.e., LH, UKIH, CM and ECK), BFI_s is the simulated BFI from the two hydrological models or the two regression approaches. And n is the total number of catchment. The unit of bias is a percentage (%). The larger the absolute bias represents the worse the simulation. The value of Bias = '0' indicates that simulation is the same as the benchmark on average.

4.2. Nash-Sutcliffe efficiency (NSE)

$$NSE = 1 \frac{\sum_{i=1}^{n} (BFI_o - BFI_s)^2}{\sum_{i=1}^{n} (BFI_o - \bar{BFI}_o)^2}$$

The Nash-Sutcliffe efficiency (NSE) is a normalized statistic that measures the relative magnitude of the residual variance ("noise") compared to the measured data variance ("information") (Nash and Sutcliffe, 1970; Gupta et al., 2009). It is a classic statistical metric used for evaluating model performance. It varies from $-\infty$ to 1, with a value close to 1 meaning a better prediction, 0 means that prediction is close to the average level of the observed value.

5. Results

5.1. Spatiality of benchmark BFI

Fig. 4 shows that benchmark BFI varies dramatically across Australia. Within latitudes 20°S and 30°S, BFI is smaller than that of the regions beyond this latitude range. Catchments located in latitudes higher than 30°S tend to have larger BFIs in general. Yet it is not the

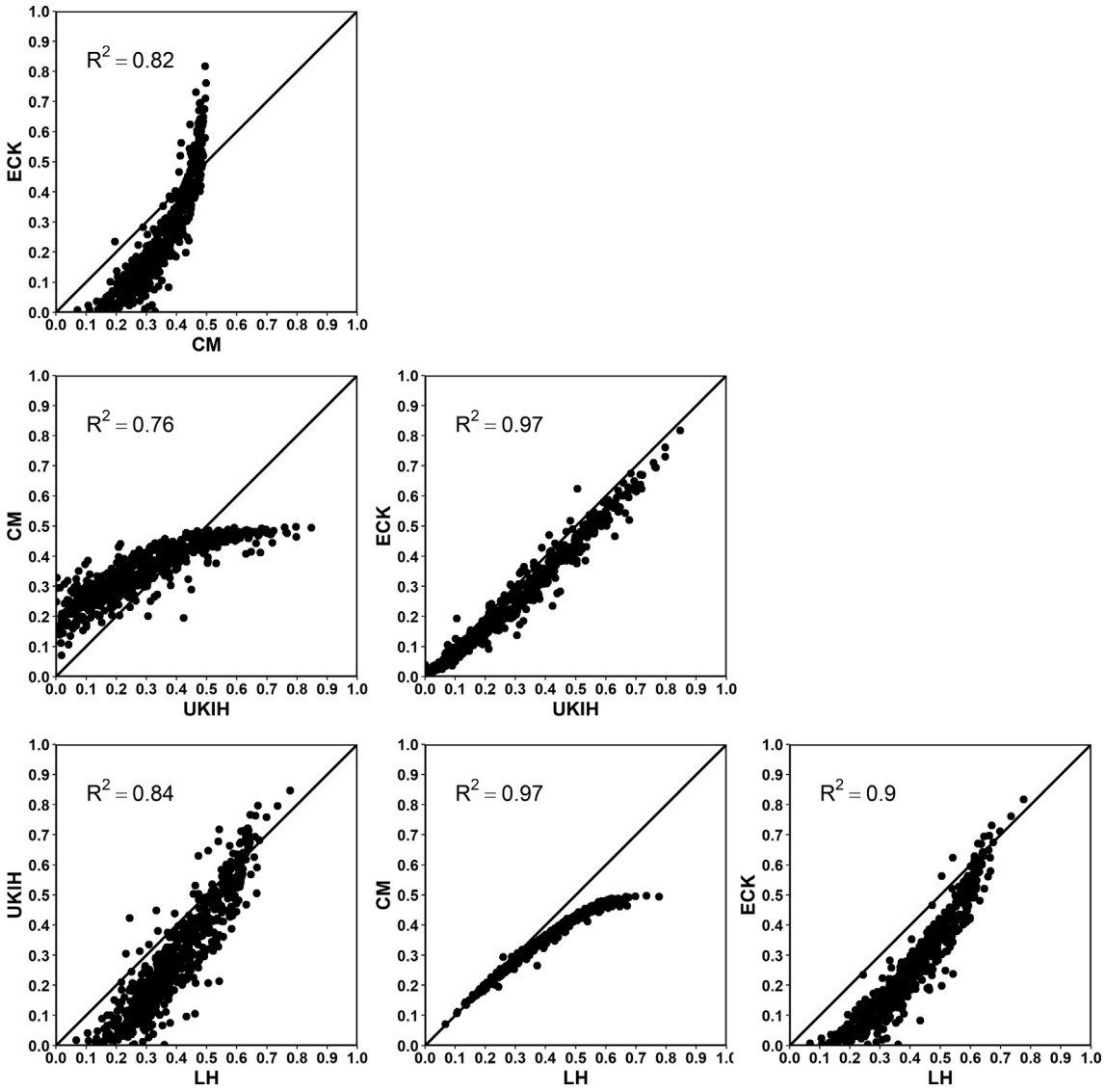

Fig. 3. Comparing baseflow index derived from four non-tracer baseflow separation methods. LH, UKIH, CM, and ECK are the baseflow index estimated from Lyne-Hollick (Lyne and Hollick, 1979), UKIH (Gustard et al., 1992), Chapman-Maxwell (Chapman and Maxwell, 1996), and Eckhardt (Eckhardt, 2005) methods.

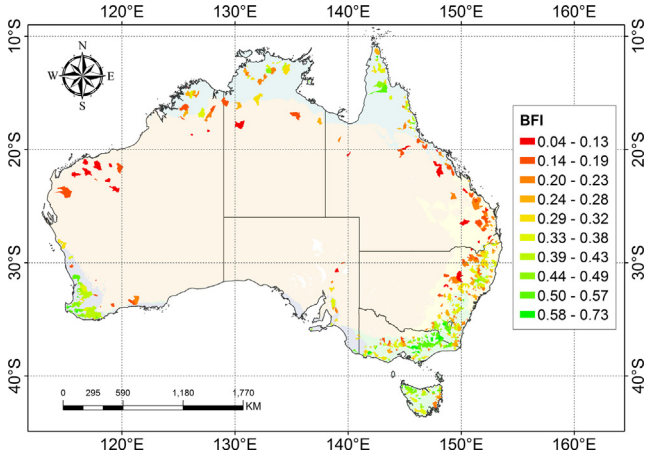

Fig. 4. Spatial distribution of the benchmark baseflow index across Australia.

case in Tasmania, where catchments with latitude higher than 40°S have smaller BFI values in the southeastern region within this island. This indicates that the BFI spatiality is distinct from the main continent to the island.

Table 3
Summary of NSE of daily runoff, NSE of daily square-root-transformed runoff (NSEsqrt) and Bias for SIMHYD and Xinanjiang models in their calibration mode.

Percentile	SIMHYD			Xinanjiang		
	NSE	NSEsqrt	Bias	NSE	NSEsqrt	Bias
10th	0.35	0.53	1	0.30	0.37	2
25th	0.50	0.65	3	0.46	0.58	3
50th	0.62	0.73	5	0.61	0.68	6
75th	0.71	0.80	8	0.71	0.76	10
90th	0.77	0.84	13	0.78	0.82	19

5.2. Performance of two hydrological models

These two hydrological models are well calibrated for 1980–2012 considering 1975 to 1979 as warm up period (Table 3). The model calibration for SIMHYD model shows that there are more than 50% catchments with NSE of daily runoff and NSE of daily square-root-

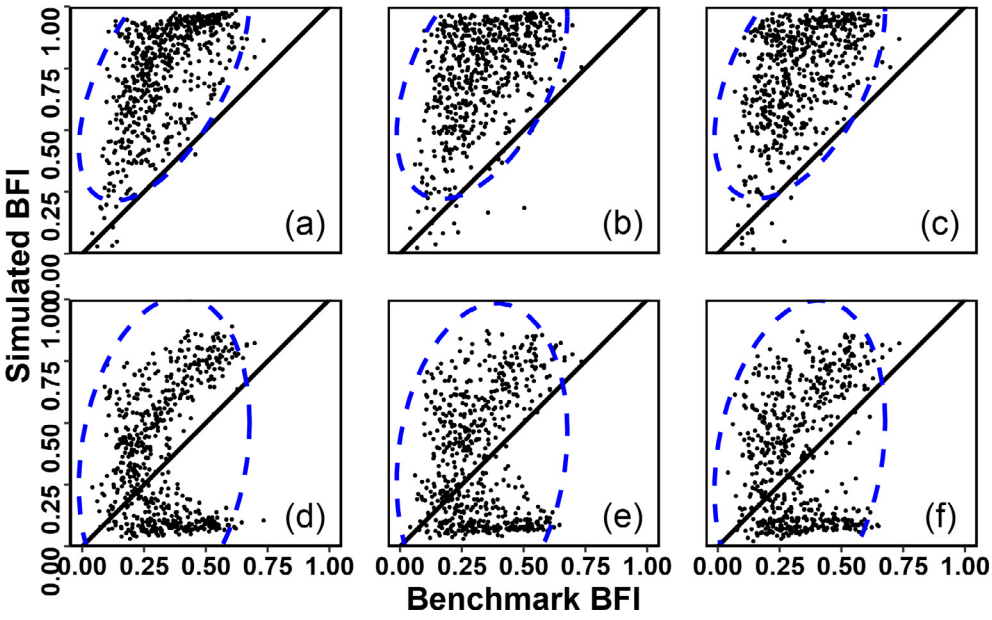

Fig. 5. Scatterplots of benchmark baseflow index versus simulated baseflow index using SIMHYD and Xinanjiang models, where calibrated and regionalised model results are presented in (a) and (d) (calibration), (b) and (e) (spatial proximity regionalisation) and (c) and (f) (integrated similarity regionalisation), respectively. The blue ellipses represent the confidence level at 0.95. SIMHYD is a simplified version of the HYDROLOG model. (For interpretation of the references to colour in this figure legend, the reader is referred to the web version of this article.)

transformed runoff data more than 0.61, and 0.73, respectively. However, the Bias between observed and simulated daily runoff is less than 5%. The model calibration for Xinanjiang model shows that there are more than 50% catchments with NSE of daily runoff and NSE of daily square-root-transformed runoff data more than 0.62 and 0.68, respectively and with Bias less than 6%.

5.3. Comparison between the benchmark and hydrological model simulated BFI

We further compared the benchmark and simulated BFI in scatterplots (Fig. 5). Fig. 5(a) and (d) compare the benchmark and simulated BFIs from calibrated SIMHYD and Xinanjiang models, respectively. Fig. 5(b)-(c) and (e)-(f) show the regionalisation results (i.e., spatial proximity and integrated similarity) of these two hydrological models. Notably, BFI estimated using SIMHYD model is much larger than the benchmark values (Fig. 5(a)–(c)), with the majority of catchment BFIs dotted above the 1:1 line. Under calibration, spatial proximity, and integrated similarity, SIMHYD model simulates BFI with NSE being −8.30, −8.42 and −8.44, respectively. The values of bias are 146%, 152% and 152%, respectively; indicating similar poor model performance. In comparison, BFI estimated from Xinanjiang model tends to scatter a larger range around 1:1 line regardless of the parameterisation method (Fig. 5(d)–(f)), and is closer to the benchmark BFI. Xinanjiang model under calibration, spatial proximity, and integrated similarity simulates BFI with NSE being −2.75, −2.70 and −2.58, respectively. The values of bias are 84%, 81% and 83%, respectively; indicating similar poor model performance in prediction of BFI.

5.4. Comparison of linear regression and multilevel regression approaches with benchmark BFI

Fig. 6 compares the benchmark BFIs and simulated BFIs using linear multivariate regression and multilevel regression approaches across four different climate zones. The best fitting equations for the traditional linear regression approach are shown in Table 4. Table 5 and Fig. 6 summarize the performance of traditional linear regression, alternative traditional regression and multilevel regression for estimating BFI in each climate zone. In calibration mode, the model performance from traditional linear regression and alternative traditional regression is very close. However, it is clear that the multilevel regression approach outperforms the linear regression approach (Table 5 and Fig. 6), with NSE for multilevel regression approach being 0.67, 0.70, and 0.72 in arid, tropics, and equiseasonal regimes, respectively. It is higher than that from linear regression. Besides, the bias from multilevel regression approach, in arid, tropics, and equiseasonal regimes are being 25%, 17%, and 19%, respectively; which are lower than that from the linear regression. The two approaches show no significant difference in winter rainfall climate zone, indicated by similar NSE and bias.

5.5. Comparison of linear regression and multilevel regression approaches using leave-one-out cross-validation

We further check the leave-one-out cross-validation results obtained from the two approaches (Fig. 7 and Table 5). It shows a higher performance from calibration to cross-validations for the traditional linear regression in arid, tropics, and equiseasonal climate zones. However, the model performance has been decreased for the alternative traditional regression. In contrast, there is no noticeable improvement for the multilevel regression approach for the three climate zones. In the winter rainfall zone, all the approaches do not have apparent improvements and perform similarly. The leave-one-out cross-validation results further demonstrate that the multilevel regression approach outperforms the linear regression. Fig. 8 further summarises predictive performances from calibration for the traditional linear regression approach in different climate zones.

5.6. Summary of the parameter values estimated for the multilevel regression approach

Fig. 9 summarises parameters of the multilevel regression approach. It is seen that P and E_{tp} have strong positive and negative effects on BFI, respectively. The mean elevation (H) and available soil water holding capacity in top soil (K_{st}) also have a noticeable positive effect in all the four climate zones. Other three characteristics area (A), mean slope (S) and forest cover ratio (F) have a slope close to zero, suggesting small impacts on BFI.

5.7. Comparison of BFI duration curves

Duration curve is a graphic method (i.e., calculative frequency curve) that can be used to elucidate the relationship between the frequency and magnitude (Kunkle, 1962; Cheng et al., 2012; Chouaib et al., 2018). Similarly, baseflow duration curve represents the baseflow

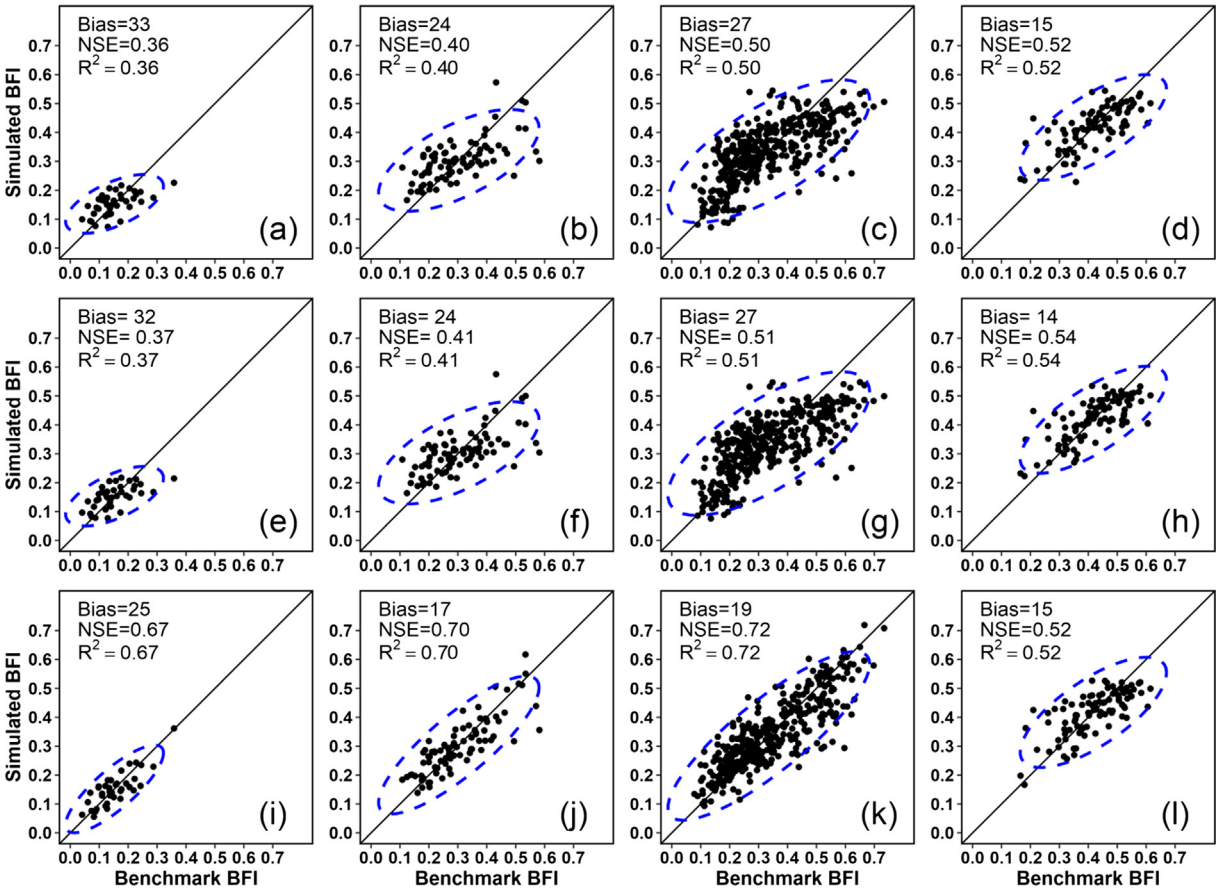

Fig. 6. Scatterplots of benchmark and simulated baseflow index using traditional linear regression ((a)-(d)), alternative traditional regression ((e)-(h)) and multilevel regression ((i)-(l)) approaches that are built using the full catchment samples in four climate zones, with (a), (e) and (i) for arid, (b), (f) and (j) for tropics, (c), (g) and (k) for equiseasonal and (d), (h) and (l) for winter rainfall, respectively. The blue ellipse is drawn at 0.95 confidence level. The black line represents 1:1 line. (For interpretation of the references to colour in this figure legend, the reader is referred to the web version of this article.)

response under underlying factors of the catchment. Fig. 10 summarises the BFI duration curves generated from the two hydrological models with three modes (calibration and two regionalisation schemes) along with linear regression and multilevel regression analysis results to compare their results with benchmark BFI. Both models, in the three parameterisation schemes, perform poorly for estimating BFI. SIMHYD model largely overestimates BFI, while the Xinanjiang model overestimates BFI at 60% catchments, and its estimated BFI is closer to the benchmark that obtained from the SIMHYD model. Differences between the calibration and two regionalisation schemes are marginal for both models. However, the two regression approaches show better performances with respect to the benchmark BFI. Particularly, multivariable regression analysis shows the best alignment among all the BFI prediction approaches.

6. Discussion

In this study, different methods (separation algorithms are applied to observed daily flow time-series) are used to gain the benchmark BFI in comparison to BFI calculation method from the process-based models (estimated using the mean annual baseflow divided by the mean annual total streamflow). Though it remains a challenge to accurately measure baseflow on a large spatial scale (Niazi et al., 2017), the benchmark BFI, however, has an apparent spatial pattern across Australia (Fig. 4). Although the benchmark BFI can be obtained through the comparison to chemical baseflow separation method, it is almost impossible to implement the chemical separations at large scale (Zhang et al., 2017). The estimation of baseflow using non-tracer method is more applicable. Since spatial pattern of BFI is consistent with streamflow recession in Australian catchments (van Dijk, 2010), it provides perspectives for understanding the dynamics of water cycle across large scales (Ahiablame et al., 2017). However, many studies have investigated the effects of catchment attributes on total streamflow (Golden et al., 2015; Woodhouse et al., 2016), but the prediction for streamflow components such as baseflow, is very limited. In this situation, the present study has been carried out.

Table 4
The traditional linear regression fitting for total dataset and sub-dataset using climate zone separately.

Climate zone	Regression equation	Number of data points
Total data	$BFI = 0.33 + 0.06P - 0.073H + 0.069F + 0.08Kst$	596
Arid	$BFI = 0.38 + 0.02A + 0.08S + 0.22P - 0.14E_{tp}$	38
Tropic	$BFI = 0.16 + 0.03A + 0.06H + 0.12P + 0.09E_{tp}$	83
Equiseasonal	$BFI = 0.27 + 0.09H + 0.05P - 0.16E_{tp} + 0.10F + 0.04K_{st}$	385
Winter rainfall	$BFI = 0.47 + 0.05A + 0.24P + 0.06F + 0.03K_{st}$	90

Table 5
Summary of BFI predictions from traditional linear regression, alternative traditional regression and multilevel regression in each climate zone. Cal and Val are denoted to the calibration and validation modes, respectively.

Methods	Traditional linear regression								Alternative traditional regression								Multilevel regression							
Climate zones	Arid		Tropic		Equiseasonal		Winter rainfall		Arid		Tropic		Equiseasonal		Winter rainfall		Arid		Tropic		Equiseasonal		Winter rainfall	
Mode	Cal	Val	Cal	Val	Cal	Val	Cal	Val	Cal	Val	Cal	Val	Cal	Val	Cal	Val	Cal	Val	Cal	Val	Cal	Val	Cal	Val
Bias	33	38	24	26	27	28	15	15	32	41	24	27	27	28	14	16	25	24	17	17	19	19	15	15
NSE	0.36	0.15	0.40	0.30	0.50	0.48	0.52	0.52	0.37	−0.04	0.41	0.25	0.54	0.48	0.51	0.44	0.67	0.70	0.70	0.70	0.72	0.72	0.52	0.52
R^2	0.36	0.19	0.40	0.31	0.50	0.48	0.52	0.52	0.37	0.08	0.41	0.27	0.54	0.48	0.51	0.44	0.67	0.70	0.70	0.70	0.72	0.72	0.52	0.52

6.1. Comparison of hydrological modelling results with benchmark BFI

Our results represent large biases in hydrological model simulations to predict BFI. It seems that model structure has a considerable effect on BFI prediction in comparison to parameter regionalisation. In fact, baseflow is designed as an integrated store combined with river recharge (Chiew and McMahon, 2002), or directly is regarded as groundwater discharge in Xinanjiang model (Li et al., 2009). Those schemes may lead to overestimating/underestimating the baseflow magnitude in some degrees. In particular, despite using similar calibration and two regionalisation schemes, SIMHYD has larger bias than Xinanjiang as summarised in Figs. 5 and 10. It is acceptable that the initial purpose of both hydrological models are to estimate streamflow and the estimations are reasonably well (NSE = 0.62 to 0.77, NSEsqrt = 0.61 to 0.78, and NSE = 0.73 to 0.84, NSEsqrt = 0.68 to 0.82 from *50*th to *90*th percentile for SIMHYD and Xinanjiang models, respectively; see Table 3). However, it is a challenge to estimate baseflow and streamflow, separately, and their proportions from a hydrological model (Fenicia et al., 2007; Lo et al., 2008). Since both hydrological models are calibrated against total daily streamflow by maximizing NSEsqrt, they can simulate and predict high streamflow well, but are not necessarily suitable for predicting low streamflow. It is possible to improve the BFI prediction accuracy by using a different calibration objective function that focuses on low streamflow, such as the NSE of reverse daily streamflow (Li and Zhang, 2017). It is possible for hydrological models to improve the BFI predictions by modifying their model structure to assimilate relative higher resolution data (i.e., remote-sensed soil moisture, actual evapotranspiration and vegetation data (Li et al., 2009; Zhang et al., 2019)). Nevertheless, this is an open question for hydrological community to answer.

6.2. Linear regression approach

The linear regression considers that the hydrological processes have a well-behaved relationship with catchment attributes (Mazvimavi et al., 2005; Gallart et al., 2007; Yao et al., 2014). However, spatial variability and complexity of underground catchment characteristics usually hamper its estimation accuracy (Oudin et al., 2008; Harman et al., 2009). This impact would be significant on a large scale but often overlooked. This suggests that linear regression can be greatly improved through reclassifying the dataset when the similar characteristics (i.e., geological classes) are properly handled (Oudin et al., 2008; Bloomfield et al., 2009; Ahiablame et al., 2017). There exists predictive performance with a higher bias for the whole dataset than the subdatasets (i.e., data from different climate regimes) for linear regression approach. Therefore, to improve our understanding for baseflow processes and BFI prediction, the interaction of catchment attributes within different climate zones should be considered (Berk and De Leeuw, 2006).

6.3. Multilevel regression approach

Interactions of catchments and different climate zones may influence the baseflow processes (Tague and Grant, 2004; Bloomfield et al., 2009). Thus, BFI is affected by catchment attributes including terrain and climate factors (Gustard and Irving, 1994; Longobardi and Villani, 2008; van Dijk, 2010; Price, 2011). Therefore, when the cross-level interactions are not strong, the benefit of using the multilevel regression approach is limited. In the winter rainfall climate zone, the linear regression and multilevel regression has performed similarly (Fig. 8). On the other hand, when the cross-level interactions are strong, the multilevel regression approach can significantly improve the BFI prediction. Thus, in the other three climate zones (Arid, Tropic, and Equiseasonal), the multilevel regression outperforms the linear regression technique. Besides, the benefit of using multilevel regression is that it considers the relationships between and within-group and it is useful

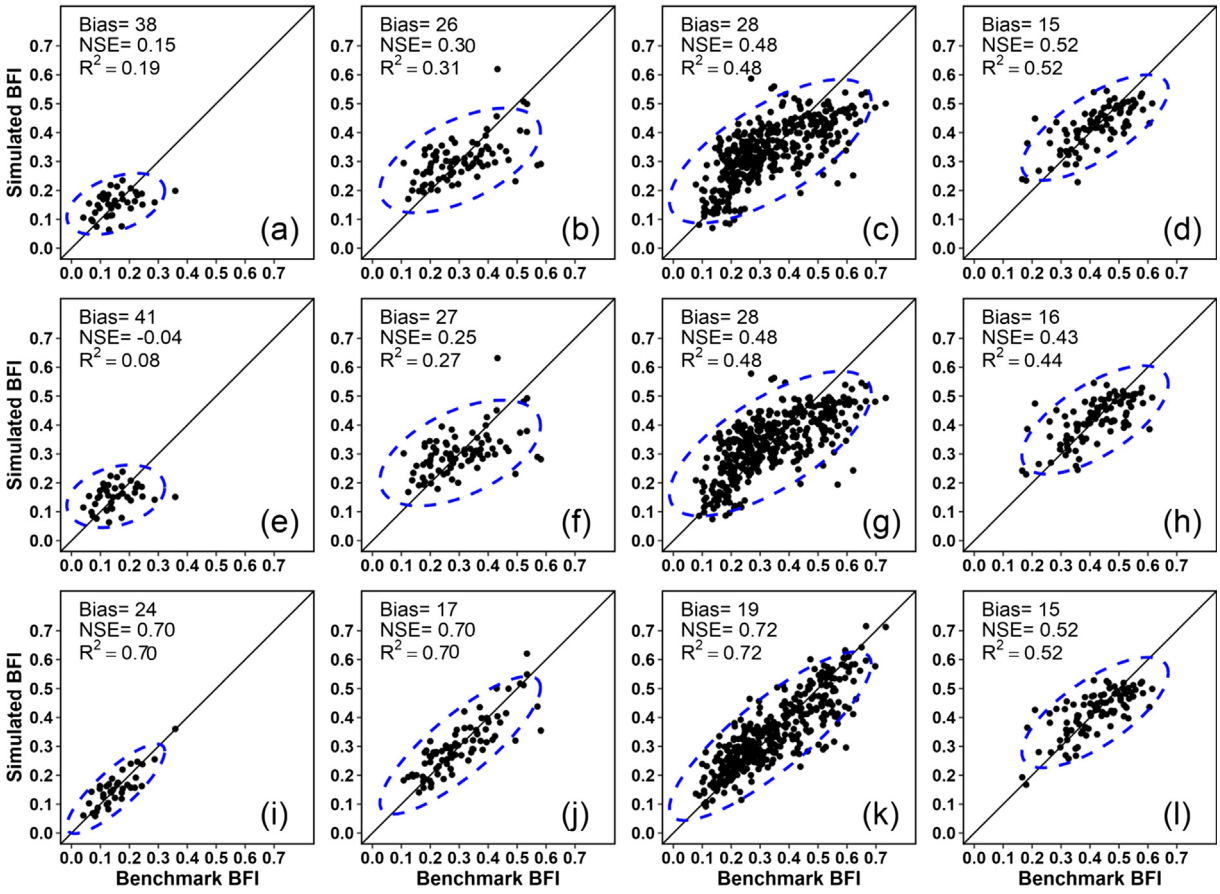

Fig. 7. As same as Fig. 7 but using the leave-one-out cross validation approach.

for uncovering the dynamics of real processes (Qian et al., 2010; Dudaniec et al., 2013). It should be noted that multilevel model (i.e., with climate classes as random effects) contain more parameters than the traditional linear regression method (with no information on climate classes). However, in this study, we focus on the models' performances rather than model parsimony. Because the parsimony of model parameters is beyond the scope of this study.

Therefore, understanding the cross-level interactions, is fundamental to elaborate the hydrological dynamics in multilevel regression technique (Qian et al., 2010). Climate factors influence the hydrological processes and lead to changes in baseflow generation. This study demonstrates that P and E_{tp} strongly influence BFI distribution and their functions vary across climate zones. Santhi et al. (2008) and Peña-Arancibia et al. (2010) have shown that climate attributes can be used to predict recession constant. Such as, the increase of precipitation can cause more frequent water saturation of the soil, and lead to increase in baseflow (Mwakalila et al., 2002; Abebe and Foerch, 2006). In general, E_{tp} is related to the baseflow discharge over the extended period (Wittenberg and Sivapalan, 1999), and has an adverse impact on BFIs (Mwakalila et al., 2002). This result agrees well with the finding from Mwakalila et al. (2002), i.e., the smaller E_{tp} impact in the arid zone than other climate zones. In comparison to P and E_{tp}, other factors show secondary or marginal impact. This is similar to the finding by Lacey and Grayson (1998) who has found that the topographic parameters have no significant relationship with BFI in southeastern Australia. However, some studies have found that S and H have a strong positive impact on the recession timescales (Peña-Arancibia et al., 2010; Krakauer and Temimi, 2011). Other studies have shown that the dominant factors influence ecological processes to vary (Berk and De Leeuw, 2006; Qian et al., 2010). But this study shows that the BFI controlling factors do not vary largely with climate regimes (Fig. 9). Traditionally, the linear regression is directly used to model the relationship between the predictors and variability; though the predictive ability is limited in lots of cases. This study has a hydrological application of the multilevel model, and demonstrates it outperforms classic linear regression when considering between and within-group interactions.

Generally, random effects should have levels that are sampled from a larger population, and the purpose is to quantify the variation among levels/units (Bolker et al., 2009). The multilevel model provides a powerful tool to solve the data that involve random effects (Bolker et al., 2009). However, climate category (number of classes = 4; names of levels meaningful) is not drawn from many classes. Thus, this may create inaccuracy in calculation as per Gelman and Hill (2006) and Harrison (2015). They recommend that multilevel models require at least 5 levels (groups) for a random intercept term to achieve robust estimates of variance. Otherwise the mixed model may not be able to estimate the among-population variance accurately (< 5 levels). In this case, the variance estimate will either collapse to zero, making the model equivalent to an ordinary generalized linear model (Gelman and Hill, 2006) or be non-zero but incorrect if the small number of groups that are sampled are not representative of the true distribution of means (Harrison, 2015). But, the low sample size (< 5 levels) in the applications of the mixed-effects models such as ecology (Harrison, 2015) has good model performance (Bolker et al., 2009). Additionally, it is also meaningful or/and reasonable that adopt four climate classes as a random effect across the Australia continent to predict BFI, and the model has an acceptable performance. Thus, this is beneficial to quantify the variation among different climate units at large scale. Nevertheless, more validations are required for using the multilevel regression approach to predict various hydrological signatures.

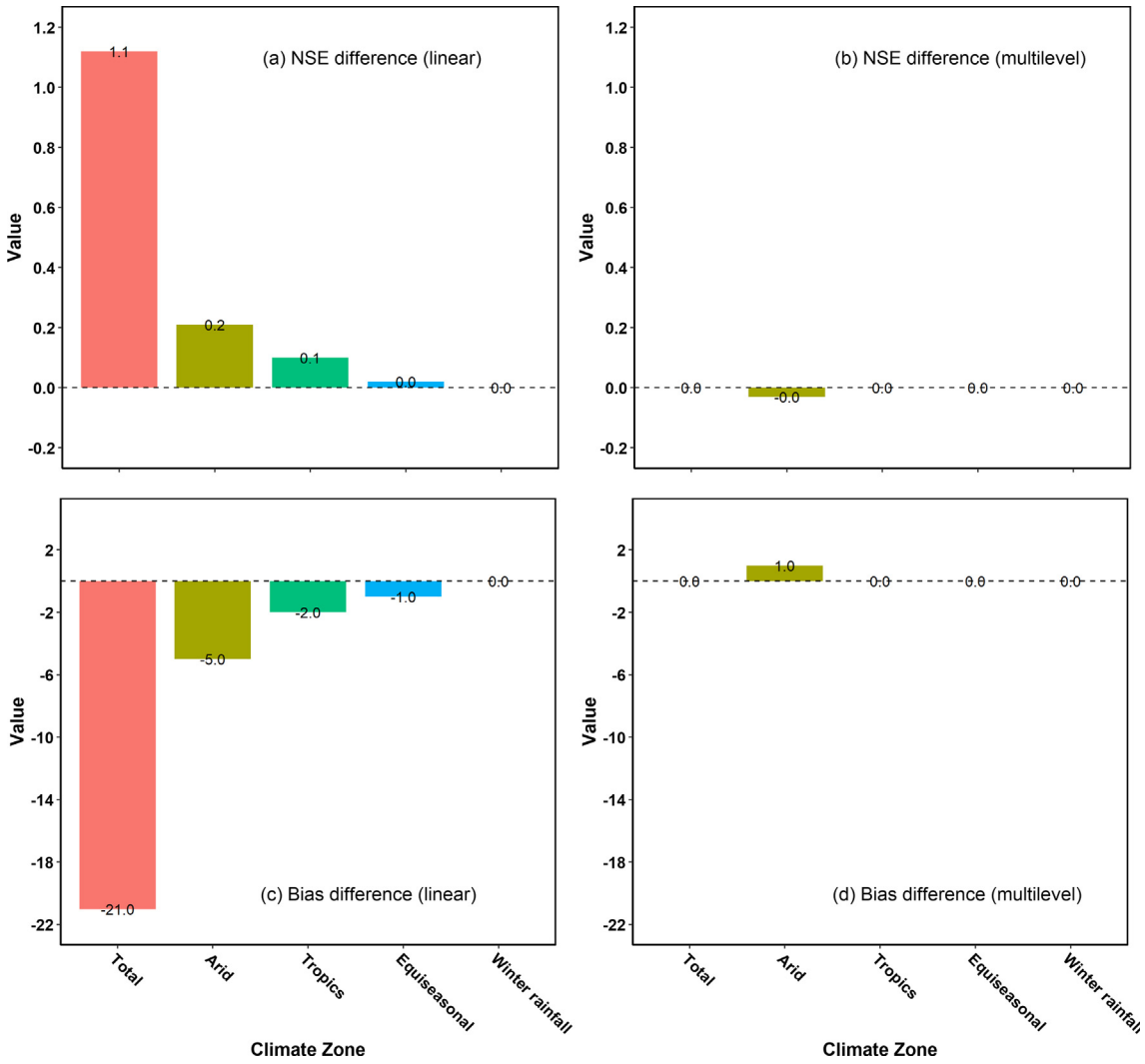

Fig. 8. The difference of NSE and the difference of Bias between calibration and validation for traditional linear regression approach ((a) and (c)) and multilevel regression approach ((b) and (d)).

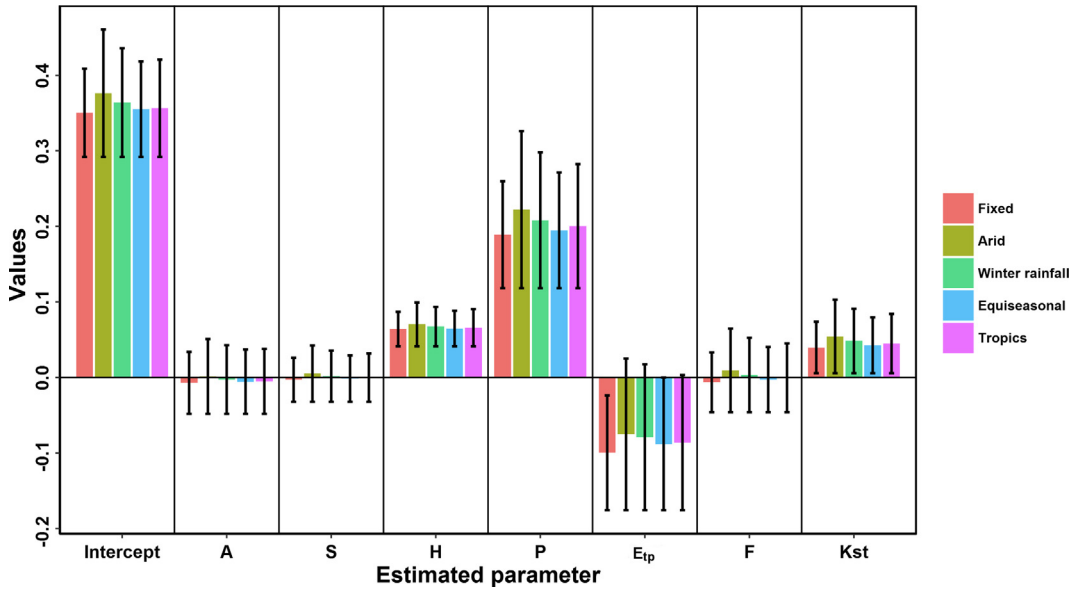

Fig. 9. Parameter values estimated for the multilevel regression approach. Error bar represents standard error of each parameter. The abbreviations of catchment attributes are introduced in Table 1.

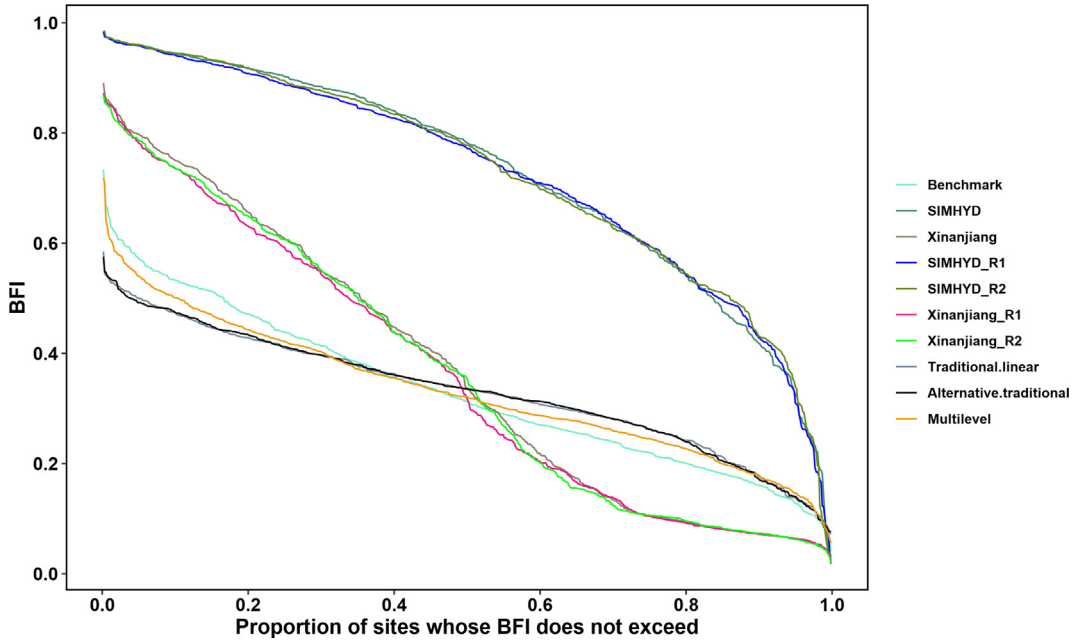

Fig. 10. Baseflow index duration curves obtained from the benchmark (mean from four non-tracer methods), SIMHYD model, Xinanjiang model, traditional linear regression, alternative traditional regression, and multilevel regression. Calibration and two regionalisation results are shown for each hydrological model, where R1 and R2 represent spatial proximity and integrated similarity approaches (mean from five donors), respectively. SIMHYD is a simplified version of the HYDROLOG model.

7. Conclusion

This study estimates combined baseflow index from four well-parameterised baseflow separation methods (LH, UKIH, CM and ECK), and finds that the baseflow index varies significantly among climate zones across the Australian continent. Multilevel regression approach is introduced to improve BFI estimation for 596 catchments across Australia, and is compared with traditional linear regression method and two hydrological models. It shows that the multilevel regression approach outperforms the linear regression approach and hydrological models. Traditional linear regression approach fails to considerate the interactions across group levels. The two hydrological models have good performance for simulating runoff yet fail to separate baseflow. In contrast, the multilevel regression approach indicates that annual precipitation, potential evapotranspiration, elevation, land cover and available soil water holding capacity in the top part of the soil-all have strong control on catchment baseflow, where climate factors such as precipitation and potential evapotranspiration are proven to be the most significant. The multilevel regression approach can provide insights into the control factors of baseflow generation, and has the potential of estimating baseflow index and other hydrological signatures in different parts of the world.

Declaration of Competing Interest

The authors declare that they have no known competing financial interests or personal relationships that could have appeared to influence the work reported in this paper.

Acknowledgments

This study was supported by CAS Pioneer Hundred Talents Program and Supporting Fund of the Institute of Geographic Sciences and Natural Resources Research, Chinese Academy of Sciences (YJRCPT2019-101), the National Natural Science Foundation of China, China (Grant Nos. 51379175 and 51679200). The first author acknowledges the Chinese Scholarship Council for supporting his PhD Study at CSIRO Land and Water. We thank Nick Potter for his comments and suggestions for an early version of this paper. We thank the Associate Editor, Eylon Shamir, and two anonymous reviewers for their critical but constructive comments. Data generated from modelling are freely available upon request from the corresponding author (Yongqiang Zhang, email: yongqiang.zhang2014@gmail.com; zhangyq@igsnrr.ac.cn). The authors declare no conflict of interest.

Declaration of Competing Interest

The authors declare that they have no conflict of interest.

References

Abdulla, F.A., Lettenmaier, D.P., Liang, X., 1999. Estimation of the ARNO model baseflow parameters using daily streamflow data. J. Hydrol. 222 (1–4), 37–54. https://doi.org/10.1016/S0022-1694(99)00096-7.

Abebe, A., Foerch, G., 2006. Catchment characteristics as predictors of base flow index (BFI) in Wabishebele river basin, east Africa. In: Conference on International Agricultural Research for Development, Siegen, Germany, pp. 1–8.

Ahiablame, L., Sheshukov, A.Y., Rahmani, V., Moriasi, D., 2017. Annual baseflow variations as influenced by climate variability and agricultural land use change in the Missouri River Basin. J. Hydrol. 551, 188–202. https://doi.org/10.1016/j.jhydrol.2017.05.055.

Arnold, J., Allen, P., Muttiah, R., Bernhardt, G., 1995. Automated base flow separation and recession analysis techniques. Groundwater 33 (6), 1010–1018. https://doi.org/10.1111/j.1745-6584.1995.tb00046.x.

Beck, H.E., van Dijk, A.I.J.M., Miralles, D.G., de Jeu, R.A.M., Sampurno Bruijnzeel, L.A., McVicar, T.R., Schellekens, J., 2013. Global patterns in base flow index and recession based on streamflow observations from 3394 catchments. Water Resour. Res. 49 (12), 7843–7863. https://doi.org/10.1002/2013wr013918.

Berk, R.A., De Leeuw, J., 2006. Multilevel Statistical Models and Ecological Scaling, Scaling and Uncertainty Analysis in Ecology. Springer, pp. 67–88.

Beven, K., Freer, J., 2001. Equifinality, data assimilation, and uncertainty estimation in mechanistic modelling of complex environmental systems using the GLUE methodology. J. Hydrol. 249 (1–4), 11–29. https://doi.org/10.1016/S0022-1694(01)00421-8.

Bloomfield, J.P., Allen, D.J., Griffiths, K.J., 2009. Examining geological controls on baseflow index (BFI) using regression analysis: an illustration from the Thames Basin, UK. J. Hydrol. 373 (1–2), 164–176. https://doi.org/10.1016/j.jhydrol.2009.04.025.

Bolker, B.M., Brooks, M.E., Clark, C.J., Geange, S.W., Poulsen, J.R., Stevens, M.H., White, J.S., 2009. Generalized linear mixed models: a practical guide for ecology and evolution. Trends Ecol. Evol. 24 (3), 127–135. https://doi.org/10.1016/j.tree.2008.10.008.

Booker, D.J., Snelder, T.H., 2012. Comparing methods for estimating flow duration curves at ungauged sites. J. Hydrol. 434–435, 78–94. https://doi.org/10.1016/j.jhydrol.2012.02.031.
Brandes, D., Hoffmann, J.G., Mangarillo, J.T., 2005. Base flow rate, low flows, and hydrologic features of small watersheds in Pennsylvania, USA. J. Am. Water Resour. Assoc. 41 (5), 1177–1186. https://doi.org/10.1111/j.1752-1688.2005.tb03792.x.
Brutsaert, W., 2005. Hydrology: An Introduction. Cambridge University Press, pp. 618.
Brutsaert, W., Lopez, J.P., 1998. Basin-scale geohydrologic drought flow features of riparian aquifers in the Southern Great Plains. Water Resour. Res. 34 (2), 233–240. https://doi.org/10.1029/97WR03068.
Brutsaert, W., Nieber, J.L., 1977. Regionalized drought flow hydrographs from a mature glaciated plateau. Water Resour. Res. 13 (3), 637–643. https://doi.org/10.1029/WR013i003p00637.
Carey, K., 2007. Modeling N2O emissions from agricultural soils using a multi-level linear regression, Citeseer.
Cawley, G.C., Talbot, N.L.C., 2003. Efficient leave-one-out cross-validation of kernel fisher discriminant classifiers. Pattern Recogn. 36 (11), 2585–2592. https://doi.org/10.1016/s0031-3203(03)00136-5.
Chapman, T., Maxwell, A., 1996. Baseflow separation-comparison of numerical methods with tracer experiments, Hydrology and Water Resources Symposium 1996: Water and the Environment; Preprints of Papers. Institution of Engineers, Australia, pp. 539.
Cheng, L., Yaeger, M., Viglione, A., Coopersmith, E., Ye, S., Sivapalan, M., 2012. Exploring the physical controls of regional patterns of flow duration curves – part 1: insights from statistical analyses. Hydrol. Earth Syst. Sci. 16 (11), 4435–4446. https://doi.org/10.5194/hess-16-4435-2012.
Cheng, L., Zhang, L., Brutsaert, W., 2016. Automated selection of pure base flows from regular daily streamflow data: objective algorithm. J. Hydrol. Eng. 21 (11), 06016008. https://doi.org/10.1061/(asce)he.1943-5584.0001427.
Cheng, L., Zhang, L., Wang, Y.-P., Canadell, J.G., Chiew, F.H.S., Beringer, J., Li, L., Miralles, D.G., Piao, S., Zhang, Y., 2017. Recent increases in terrestrial carbon uptake at little cost to the water cycle. Nature Commun. 8 (1). https://doi.org/10.1038/s41467-017-00114-5.
Chiew, F., McMahon, T., 1994. Application of the daily rainfall-runoff model MODHYDROLOG to 28 Australian catchments. J. Hydrol. 153 (1), 383–416. https://doi.org/10.1016/0022-1694(94)90200-3.
Chiew, F.H.S., McMahon, T.A., 2002. Modelling the impacts of climate change on Australian streamflow. Hydrol. Processes 16 (6), 1235–1245. https://doi.org/10.1002/hyp.1059.
Chiew, F.H.S., Teng, J., Vaze, J., Post, D.A., Perraud, J.M., Kirono, D.G.C., Viney, N.R., 2009. Estimating climate change impact on runoff across southeast Australia: method, results, and implications of the modeling method. Water Resour. Res. 45 (10), W10414. https://doi.org/10.1029/2008wr007338.
Chouaib, W., Caldwell, P.V., Alila, Y., 2018. Regional variation of flow duration curves in the eastern United States: process-based analyses of the interaction between climate and landscape properties. J. Hydrol. 559, 327–346. https://doi.org/10.1016/j.jhydrol.2018.01.037.
Dudaniec, R.Y., Rhodes, J.R., Worthington Wilmer, J., Lyons, M., Lee, K.E., McAlpine, C.A., Carrick, F.N., 2013. Using multilevel models to identify drivers of landscape-genetic structure among management areas. Mol. Ecol. 22 (14), 3752–3765. https://doi.org/10.1111/mec.12359.
Eckhardt, K., 2005. How to construct recursive digital filters for baseflow separation. Hydrol. Processes 19 (2), 507–515. https://doi.org/10.1002/hyp.5675.
Fenicia, F., Savenije, H.H.G., Matgen, P., Pfister, L., 2007. A comparison of alternative multiobjective calibration strategies for hydrological modeling. Water Resour. Res. 43 (3), W03434. https://doi.org/10.1029/2006WR005098.
Ferket, B.V.A., Samain, B., Pauwels, V.R.N., 2010. Internal validation of conceptual rainfall–runoff models using baseflow separation. J. Hydrol. 381 (1–2), 158–173. https://doi.org/10.1016/j.jhydrol.2009.11.038.
Friedl, M., Strahler, A., Hodges, J., 2010. ISLSCP II MODIS (Collection 4) IGBP Land Cover, 2000–2001. ISLSCP Initiative II Collection. Data set. Available on-line [http://daac. ornl. gov/] from Oak Ridge National Laboratory Distributed Active Archive Center, Oak Ridge, Tennessee, USA, 10. DOI:10.3334/ORNLDAAC/968.
Furey, P.R., Gupta, V.K., 2001. A physically based filter for separating base flow from streamflow time series. Water Resour. Res. 37 (11), 2709–2722. https://doi.org/10.1029/2001wr000243.
Gallart, F., Latron, J., Llorens, P., Beven, K., 2007. Using internal catchment information to reduce the uncertainty of discharge and baseflow predictions. Adv. Water Res. 30 (4), 808–823. https://doi.org/10.1016/j.advwatres.2006.06.005.
Gebert, W.A., Radloff, M.J., Considine, E.J., Kennedy, J.L., 2007. Use of streamflow data to estimate base flow/ground-water recharge For Wisconsin1. JAWRA J. Am. Water Resour. Assoc. 43 (1), 220–236. https://doi.org/10.1111/j.1752-1688.2007.00018.x.
Gelman, A., Hill, J., 2006. Data Analysis Using Regression and Multilevel/Hierarchical Models. Cambridge University Press.
Golden, H., Sander, H., Lane, R.C., Zhao, C., Price, K., D'Amico, E.R., Christensen, J., 2015. Relative effects of geographically isolated wetlands on streamflow: a watershed-scale analysis. Ecohydrology 9 (1), 21–38. https://doi.org/10.1002/eco.1608.
Gonzales, A., Nonner, J., Heijkers, J., Uhlenbrook, S., 2009. Comparison of different base flow separation methods in a lowland catchment. Hydrol. Earth Syst. Sci. 13 (11), 2055–2068. https://doi.org/10.5194/hess-13-2055-2009.
Granados, V., Gutiérrez-Cánovas, C., Arias-Real, R., Obrador, B., Harjung, A., Butturini, A., 2020. The interruption of longitudinal hydrological connectivity causes delayed responses in dissolved organic matter. Sci. Total Environ. 713, 136619. https://doi.org/10.1016/j.scitotenv.2020.136619.
Gupta, H.V., Kling, H., Yilmaz, K.K., Martinez, G.F., 2009. Decomposition of the mean squared error and NSE performance criteria: implications for improving hydrological modelling. J. Hydrol. 377 (1–2), 80–91. https://doi.org/10.1016/j.jhydrol.2009.08.003.
Gustard, A., Irving, K., 1994. Classification of the low flow response of European soils. IAHS Publications-Series of Proceedings and Reports-Intern Assoc Hydrological Sciences, 221: 113–118.
Gustard, A., Bullock, A., Dixon, J., 1992. Low Flow Estimation in the United Kingdom. Institute of Hydrology.
Gusyev, M.A., Morgenstern, U., Stewart, M.K., Yamazaki, Y., Kashiwaya, K., Nishihara, T., Kuribayashi, D., Sawano, H., Iwami, Y., 2016. Application of tritium in precipitation and baseflow in Japan: a case study of groundwater transit times and storage in Hokkaido watersheds. Hydrol. Earth Syst. Sci. 20 (7), 3043–3058. https://doi.org/10.5194/hess-20-3043-2016.
Haberlandt, U., Klöcking, B., Krysanova, V., Becker, A., 2001. Regionalisation of the base flow index from dynamically simulated flow components — a case study in the Elbe River Basin. J. Hydrol. 248 (1–4), 35–53. https://doi.org/10.1016/S0022-1694(01)00391-2.
Harman, C.J., Sivapalan, M., Kumar, P., 2009. Power law catchment-scale recessions arising from heterogeneous linear small-scale dynamics. Water Resour. Res. 45 (9). https://doi.org/10.1029/2008wr007392.
Harrison, X.A., 2015. A comparison of observation-level random effect and Beta-Binomial models for modelling overdispersion in Binomial data in ecology & evolution. PeerJ 3, e1114. https://doi.org/10.7717/peerj.1114.
Jeffrey, S.J., Carter, J.O., Moodie, K.B., Beswick, A.R., 2001. Using spatial interpolation to construct a comprehensive archive of Australian climate data. Environ. Model. Software 16 (4), 309–330. https://doi.org/10.1016/S1364-8152(01)00008-1.
Jung, M., Reichstein, M., Ciais, P., Seneviratne, S.I., Sheffield, J., Goulden, M.L., Bonan, G., Cescatti, A., Chen, J., de Jeu, R., Dolman, A.J., Eugster, W., Gerten, D., Gianelle, D., Gobron, N., Heinke, J., Kimball, J., Law, B.E., Montagnani, L., Mu, Q., Mueller, B., Oleson, K., Papale, D., Richardson, A.D., Roupsard, O., Running, S., Tomelleri, E., Viovy, N., Weber, U., Williams, C., Wood, E., Zaehle, S., Zhang, K., 2010. Recent decline in the global land evapotranspiration trend due to limited moisture supply. Nature 467 (7318), 951–954. https://doi.org/10.1038/nature09396.
Knisel, W.G., 1963. Baseflow recession analysis for comparison of drainage basins and geology. J. Geophys. Res. 68 (12), 3649–3653. https://doi.org/10.1029/JZ068i012p03649.
Koskelo, A.I., Fisher, T.R., Utz, R.M., Jordan, T.E., 2012. A new precipitation-based method of baseflow separation and event identification for small watersheds (< 50km2). J. Hydrol. 450–451, 267–278. https://doi.org/10.1016/j.jhydrol.2012.04.055.
Kottek, M., Grieser, J., Beck, C., Rudolf, B., Rubel, F., 2006. World Map of the Köppen-Geiger climate classification updated. Meteorol. Z. 15 (3), 259–263. https://doi.org/10.1127/0941-2948/2006/0130.
Krakauer, N.Y., Temimi, M., 2011. Stream recession curves and storage variability in small watersheds. Hydrol. Earth Syst. Sci. 15 (7), 2377–2389. https://doi.org/10.5194/hess-15-2377-2011.
Kunkle, G.R., 1962. The baseflow-duration curve, a technique for the study of groundwater discharge from a drainage basin. J. Geophys. Res. 67 (4), 1543–1554. https://doi.org/10.1029/JZ067i004p01543.
Lacey, G.C., Grayson, R.B., 1998. Relating baseflow to catchment properties in south-eastern Australia. J. Hydrol. 204 (1–4), 231–250. https://doi.org/10.1016/S0022-1694(97)00124-8.
Lambert, J., Gong, L., Elliott, C.F., Thompson, K., Stromberg, A.J.R.J., 2018. rFSA: an R Package for Finding Best Subsets and Interactions. R J. 10 (2).
Leuning, R., Zhang, Y.Q., Rajaud, A., Cleugh, H., Tu, K., 2009. Correction to "A simple surface conductance model to estimate regional evaporation using MODIS leaf area index and the Penman-Monteith equation". Water Resour. Res. 45 (1), W01701. https://doi.org/10.1029/2008wr007631.
Li, H., Zhang, Y., 2016. Regionalising rainfall–runoff modelling for predicting daily runoff in continental Australia. Hydrol. Earth Syst. Sci. Discuss. 1–24. https://doi.org/10.5194/hess-2016-464.
Li, H., Zhang, Y., 2017. Regionalising rainfall-runoff modelling for predicting daily runoff: comparing gridded spatial proximity and gridded integrated similarity approaches against their lumped counterparts. J. Hydrol. 550, 279–293. https://doi.org/10.1016/j.jhydrol.2017.05.015.
Li, H., Zhang, Y., Chiew, F.H.S., Xu, S., 2009. Predicting runoff in ungauged catchments by using Xinanjiang model with MODIS leaf area index. J. Hydrol. 370 (1–4), 155–162. https://doi.org/10.1016/j.jhydrol.2009.03.003.
Lo, M.-H., Yeh, P.J.F., Famiglietti, J.S., 2008. Constraining water table depth simulations in a land surface model using estimated baseflow. Adv. Water Res. 31 (12), 1552–1564. https://doi.org/10.1016/j.advwatres.2008.06.007.
Longobardi, A., Villani, P., 2008. Baseflow index regionalization analysis in a mediterranean area and data scarcity context: role of the catchment permeability index. J. Hydrol. 355 (1–4), 63–75. https://doi.org/10.1016/j.jhydrol.2008.03.011.
Lott, D.A., Stewart, M.T., 2016. Base flow separation: a comparison of analytical and mass balance methods. J. Hydrol. 535, 525–533. https://doi.org/10.1016/j.jhydrol.2016.01.063.
Lü, H., Hou, T., Horton, R., Zhu, Y., Chen, X., Jia, Y., Wang, W., Fu, X., 2013. The streamflow estimation using the Xinanjiang rainfall runoff model and dual state-parameter estimation method. J. Hydrol. 480, 102–114. https://doi.org/10.1016/j.jhydrol.2012.12.011.
Luo, Y., Arnold, J., Allen, P., Chen, X., 2012. Baseflow simulation using SWAT model in an inland river basin in Tianshan Mountains, Northwest China. Hydrol. Earth Syst. Sci. 16 (4), 1259–1267. https://doi.org/10.5194/hess-16-1259-2012.
Luo, Z., Wang, E., Smith, C., 2015. Fresh carbon input differentially impacts soil carbon decomposition across natural and managed systems. Ecology 96 (10), 2806–2813. https://doi.org/10.1890/14-2228.1.

Lyne, V., Hollick, M., 1979. Stochastic time-variable rainfall-runoff modelling. Inst. Eng. Aust. Natl. Conf. 89–93.
MathWorks, T., 2006. Genetic algorithm and direct search toolbox 2 user's guide, pp. 5. 2–5.13, Natick, Mass.
Mazvimavi, D., Meijerink, A.M.J., Savenije, H.H.G., Stein, A., 2005. Prediction of flow characteristics using multiple regression and neural networks: a case study in Zimbabwe. Phys. Chem. Earth, Parts A/B/C 30 (11–16), 639–647. https://doi.org/10.1016/j.pce.2005.08.003.
McMahon, S.M., Diez, J.M., 2007. Scales of association: hierarchical linear models and the measurement of ecological systems. Ecol. Lett. 10 (6), 437–452. https://doi.org/10.1111/j.1461-0248.2007.01036.x.
Meynink, W., 2011. Modelling equatorial baseflow. In: Proceedings of the 34th World Congress of the International Association for Hydro-Environment Research and Engineering: 33rd Hydrology and Water Resources Symposium and 10th Conference on Hydraulics in Water Engineering. Engineers Australia, pp. 1419.
Miller, M.P., Susong, D.D., Shope, C.L., Heilweil, V.M., Stolp, B.J., 2014. Continuous estimation of baseflow in snowmelt-dominated streams and rivers in the Upper Colorado River Basin: a chemical hydrograph separation approach. Water Resour. Res. 50 (8), 6986–6999. https://doi.org/10.1002/2013WR014939.
Miller, M.P., Buto, S.G., Susong, D.D., Rumsey, C.A., 2016. The importance of base flow in sustaining surface water flow in the Upper Colorado River Basin. Water Resour. Res. 52 (5), 3547–3562. https://doi.org/10.1002/2015WR017963.
Mwakalila, S., Feyen, J., Wyseure, G., 2002. The influence of physical catchment properties on baseflow in semi-arid environments. J. Arid Environ. 52 (2), 245–258. https://doi.org/10.1006/jare.2001.0947.
Nash, J.E., Sutcliffe, J.V., 1970. River flow forecasting through conceptual models part I — a discussion of principles. J. Hydrol. 10 (3), 282–290. https://doi.org/10.1016/0022-1694(70)90255-6.
Niazi, A., Bentley, L.R., Hayashi, M., 2017. Estimation of spatial distribution of groundwater recharge from stream baseflow and groundwater chloride. J. Hydrol. 546, 380–392. https://doi.org/10.1016/j.jhydrol.2017.01.032.
Oudin, L., Andréassian, V., Perrin, C., Michel, C., Le Moine, N., 2008. Spatial proximity, physical similarity, regression and ungaged catchments: a comparison of regionalization approaches based on 913 French catchments. Water Resour. Res. 44 (3), W03413. https://doi.org/10.1029/2007wr006240.
Partington, D., Brunner, P., Simmons, C.T., Werner, A.D., Therrien, R., Maier, H.R., Dandy, G.C., 2012. Evaluation of outputs from automated baseflow separation methods against simulated baseflow from a physically based, surface water-groundwater flow model. J. Hydrol. 458–459, 28–39. https://doi.org/10.1016/j.jhydrol.2012.06.029.
Peña-Arancibia, J.L., van Dijk, A.I.J.M., Mulligan, M., Bruijnzeel, L.A., 2010. The role of climatic and terrain attributes in estimating baseflow recession in tropical catchments. Hydrol. Earth Syst. Sci. 14 (11), 2193–2205. https://doi.org/10.5194/hess-14-2193-2010.
Piggott, A.R., Moin, S., Southam, C., 2005. A revised approach to the UKIH method for the calculation of baseflow. Hydrol. Sci. J. 50 (5). https://doi.org/10.1623/hysj.2005.50.5.911.
Price, K., 2011. Effects of watershed topography, soils, land use, and climate on baseflow hydrology in humid regions: a review. Prog. Phys. Geogr. 35 (4), 465–492. https://doi.org/10.1177/0309133311402714.
Qian, S.S., Cuffney, T.F., Alameddine, I., McMahon, G., Reckhow, K.H., 2010. On the application of multilevel modeling in environmental and ecological studies. Ecology 91 (2), 355–361. https://doi.org/10.1890/09-1043.1.
Reynolds, L.V., Shafroth, P.B., LeRoy Poff, N., 2015. Modeled intermittency risk for small streams in the Upper Colorado River Basin under climate change. J. Hydrol. 523, 768–780. https://doi.org/10.1016/j.jhydrol.2015.02.025.
Rice, K.C., Hornberger, G.M., 1998. Comparison of hydrochemical tracers to estimate source contributions to peak flow in a small, forested, headwater catchment. Water Resour. Res. 34 (7), 1755–1766. https://doi.org/10.1029/98WR00917.
Santhi, C., Allen, P.M., Muttiah, R.S., Arnold, J.G., Tuppad, P., 2008. Regional estimation of base flow for the conterminous United States by hydrologic landscape regions. J. Hydrol. 351 (1–2), 139–153. https://doi.org/10.1016/j.jhydrol.2007.12.018.
Spongberg, M., 2000. Spectral analysis of base flow separation with digital filters. Water Resour. Res. 36 (3), 745–752. https://doi.org/10.1029/1999WR900303.
Stoelzle, M., Weiler, M., Stahl, K., Morhard, A., Schuetz, T., 2015. Is there a superior conceptual groundwater model structure for baseflow simulation? Hydrol. Processes 29 (6), 1301–1313. https://doi.org/10.1002/hyp.10251.
Tague, C., Grant, G.E., 2004. A geological framework for interpreting the low-flow regimes of Cascade streams, Willamette River Basin. Oregon. Water Resour. Res. 40 (4), W04303. https://doi.org/10.1029/2003wr002629.
Tularam, G.A., Ilahee, M., 2008. Exponential smoothing method of base flow separation and its impact on continuous loss estimates. Am. J. Environ. Sci. 4 (4), 373–381. https://doi.org/10.3844/ajessp.2008.136.144.
van Dijk, A.I.J.M., 2010. Climate and terrain factors explaining streamflow response and recession in Australian catchments. Hydrol. Earth Syst. Sci. 14 (1), 159–169. https://doi.org/10.5194/hess-14-159-2010.
Vaze, J., Teng, J., 2011. Future climate and runoff projections across New South Wales, Australia: results and practical applications. Hydrol. Processes 25 (1), 18–35. https://doi.org/10.1002/hyp.7812.
Viney, N.R., McMahon, T.A., Chiew, F.H.S., 2011. Guidelines for Presentation of the Bureau of Meteorology National Streamflow Database. CSIRO: Water for a Healthy Country. National Research Flagship, pp. 46.
Wasserman, G.S., Sudjianto, A., 1994. All subsets regression using a genetic search algorithm. Comput. Ind. Eng. 27 (1), 489–492. https://doi.org/10.1016/0360-8352(94)90341-7.
Wittenberg, H., Sivapalan, M., 1999. Watershed groundwater balance estimation using streamflow recession analysis and baseflow separation. J. Hydrol. 219 (1), 20–33. https://doi.org/10.1016/S0022-1694(99)00040-2.
A. Woodhouse, C., Pederson, G., Morino, K., McAfee, S., McCabe, G., 2016. Increasing influence of air temperature on upper Colorado River streamflow. 43: 2174–2181. DOI:10.1002/2015GL067613.
Yao, C., Zhang, K., Yu, Z., Li, Z., Li, Q., 2014. Improving the flood prediction capability of the Xinanjiang model in ungauged nested catchments by coupling it with the geomorphologic instantaneous unit hydrograph. J. Hydrol. 517, 1035–1048. https://doi.org/10.1016/j.jhydrol.2014.06.037.
Zhang, Y., Chiew, F.H.S., 2009. Relative merits of different methods for runoff predictions in ungauged catchments. Water Resour. Res. 45 (7), W07412. https://doi.org/10.1029/2008wr007504.
Zhang, Y., Ahiablame, L., Engel, B., Liu, J., 2013a. Regression modeling of baseflow and baseflow index for Michigan USA. Water 5 (4), 1797–1815. https://doi.org/10.3390/w5041797.
Zhang, Y., Viney, N., Frost, A., Oke, A., Brooks, M., Chen, Y., Campbell, N., 2013. Collation of Australian modeller's streamflow dataset for 780 unregulated Australian catchments. Water for a Healthy Country National Research Flagship, 115 pp. Catchment Management. DOI:10.4225/08/58b5baad4fcc2.
Zhang, Y., Leuning, R., Hutley, L.B., Beringer, J., McHugh, I., Walker, J.P., 2010. Using long-term water balances to parameterize surface conductances and calculate evaporation at 0.05° spatial resolution. Water Resour. Res. 46 (5), W05512. https://doi.org/10.1029/2009wr008716.
Zhang, Y., Vaze, J., Chiew, F.H.S., Teng, J., Li, M., 2014. Predicting hydrological signatures in ungauged catchments using spatial interpolation, index model, and rainfall–runoff modelling. J. Hydrol. 517, 936–948. https://doi.org/10.1016/j.jhydrol.2014.06.032.
Zhang, Y., Zheng, H., Chiew, F.H.S., Arancibia, J.P., Zhou, X., 2016. Evaluating regional and global hydrological models against streamflow and evapotranspiration measurements. J. Hydrometeorol. 17 (3), 995–1010. https://doi.org/10.1175/jhm-d-15-0107.1.
Zhang, Y., Chiew, F.H.S., Li, M., Post, D., 2018. Predicting runoff signatures using regression and hydrological modeling approaches. Water Resour. Res. 54 (10), 7859–7878. https://doi.org/10.1029/2018wr023325.
Zhang, Y., Kong, D., Gan, R., Chiew, F.H.S., McVicar, T.R., Zhang, Q., Yang, Y., 2019. Coupled estimation of 500 m and 8-day resolution global evapotranspiration and gross primary production in 2002–2017. Remote Sens. Environ. 222, 165–182. https://doi.org/10.1016/j.rse.2018.12.031.
Zhang, J., Zhang, Y., Song, J., Cheng, L., 2017. Evaluating relative merits of four baseflow separation methods in Eastern Australia. J. Hydrol. 549 (2017), 252–263. https://doi.org/10.1016/j.jhydrol.2017.04.004.
Zhao, R.J., 1992. The Xinanjiang model applied in China. J. Hydrol. 135 (1), 371–381. https://doi.org/10.1016/0022-1694(92)90096-E.
Zhu, Z., Bi, J., Pan, Y., Ganguly, S., Anav, A., Xu, L., Samanta, A., Piao, S., Nemani, R., Myneni, R., 2013. Global Data Sets of Vegetation Leaf Area Index (LAI)3g and Fraction of Photosynthetically Active Radiation (FPAR)3g Derived from Global Inventory Modeling and Mapping Studies (GIMMS) Normalized Difference Vegetation Index (NDVI3g) for the Period 1981 to 2011. Remote Sens. 5 (2), 927–948. https://doi.org/10.3390/rs5020927.